Free-Vibration of Adaptive Sandwich Composite Beams with Piezoelectric Actuators and Sensors Using Coupled High-Order Layerwise Mechanics

Theofanis S. Plagianakos[1] and Dimitris A. Saravanos[2]
Department of Mechanical Engineering and Aeronautics
University of Patras, Patras, GR 26500
Greece

ABSTRACT

A high-order discrete layer theoretical framework and a finite element are presented for predicting the damped dynamic response of sandwich beams with piezoelectric layers. A new layerwise coupled piezoelectric laminate theory is developed, in which quadratic and cubic fields are added to the in-plane displacement and electric potential approximation in each discrete layer, moreover interlaminar shear stress continuity is imposed through the thickness. A beam finite element is further developed and used to predict the coupled electromechanical damped dynamic behaviour of a sandwich beam with piezoelectric layers. Comparisons with linear layerwise beam finite element predictions illustrate the accuracy and capability of the developed mechanics to efficiently capture the global and local response of smart piezoelectric composite sandwich beams. The enhancement of damping by addition of interlaminar compliant layers between an active restraining piezoelectric layer and the composite face laminate is studied.

1. INTRODUCTION

Multi-functional smart sandwich structures with composite faces, foam cores and embedded piezoelectric actuators and sensors will combine the excellent mechanical properties of sandwich structures, e.g. high flexural stiffness and strength to mass ratio and higher damping, with the additional capabilities to sense deformation and stress states and to adapt their response accordingly. Yet, such structures are challenging to model and analyze due to the inhomogeneity in properties and anisotropy through the thickness, the high thickness of the laminate and the shearing of the core, which all affect their electromechanical response.

The analysis of smart sandwich structures can be best accomplished by discrete-layer theories which effectively describe the discontinuities in the slopes of displacement and electric potential field through the thickness. Various coupled laminate theories and finite element models with linear layerwise approximations [1, 2] and exact solutions [3,4] have been presented, which predict the electromechanical response of composite beams and plates with active or sensory piezoelectric layers or patches. Coupled mixed-field theories and finite element methods for smart composite shell structures have also been derived [5]. Gu et al [6] applied a layerwise displacement field with a continuous cubic distribution through the thickness and a layerwise linear potential field and presented a finite element solution for the coupled thermo-piezoelectric response of plates; whereas, Kim et al. [7] further assumed a higher order electric potential field through the thickness and studied stress and temperature distributions through the thickness of shell structures with a piezoelectric patch under thermal loading. Cho and Oh presented an analytical solution [8], assuming a smooth cubic displacement field through the thickness, on which a linear layerwise displacement field was superimposed, and a layerwise linear potential field to study the through-thickness thermo-piezoelectric response of plates under combined loading. In the area of adaptive sandwich beams, various Ritz-type solutions [9] and finite elements [10, 11] have been presented for studying their static and modal response under extensional or shear actuation, assuming a linear displacement and electric potential field through the thickness of each face and the core. Vel and Batra [12] presented an analytical solution with layerwise linear approximation of displacement and electric potential for adaptive sandwich plates with piezoelectric shear actuators.

---

[1] Postgraduate Student
[2] Associate Professor, e-mail: saravanos@mech.upatras.gr

The present paper presents a layerwise theory which admits high-order displacement and electric potential fields in each discrete layer. In the following paragraphs, the new high-order kinematic approximations of displacement and electric fields are described. They are combined with the coupled equations of motion to yield stiffness, piezoelectric, permittivity, mass and viscoelastic damping matrices from ply to laminate level. The higher order terms are additional elastic or electric degrees of freedom of the piezoelectric laminate, with respect to the field they describe. Interlaminar shear stress compatibility conditions are subsequently imposed, leading to a reduction of the laminate matrices and improved stress and strain predictions. A beam finite element is further developed incorporating the aforementioned piezoelectric theory, and structural matrices are formed. The local and global modal response of a sandwich composite beam with piezoelectric layers is compared with coupled linear layerwise finite element predictions. The effect of viscoelastic constrained damping layers is predicted and the option to actively increase shear damping in the constrained layer by proper feedback on the actuator voltage is investigated.

2. THEORETICAL FORMULATION

The next few paragraphs describe the integrated theoretical framework, starting from material level and arriving to the prediction of the coupled piezoelectric response.

Governing Material Equations. Each ply is assumed to exhibit linear piezoelectric behavior. The constitutive equations have the form:

$$\begin{aligned} \sigma_{c_i} &= (Q_{c_{ij}}{}^{E} + jQ_{c_{in}}\eta^{E}{}_{c_{nj}})S_{c_j} - e_{ik}E_k \\ D_m &= e_{mj}S_{c_j} + \varepsilon^{S}_{mk}E_k \end{aligned} \tag{1}$$

where i,j,n=1,…,6 and k,m=1,…,3; σ_{c_i} and S_{c_j} are the mechanical stresses and engineering strains in vectorial notation, subscript c indicates the structural coordinate system Oxyz and is implied in the following paragraphs; j is the imaginary unit; E_m is the electric field vector; D_m is the electric displacement vector; $Q_{c_{ij}}$ is the elastic stiffness tensor; e_{lk} is the piezoelectric tensor; and ε_{mk} is the electric permittivity tensor of the material; $\eta_{c_{ij}}$ is the off-axis loss factor matrix. Superscripts E and S indicate constant electric field and strain conditions, respectively. The loss factor matrix is related through a proper rotational transformation to the on-axis damping matrix $[\eta_l]$ containing the four independent damping loss factors of a composite ply, describing the longitudinal damping η_{l1} (direction 11), transverse damping η_{l2} (direction 22), in plane shear damping $\eta_{l6} = \eta_{l5}$ (directions 12 and 13) and interlaminar shear damping η_{l4} (direction 23). The above equations may encompass the behaviour of both an off-axis homogenized fibrous piezoelectric ply and a passive composite ply ($[e]=0$).

Equations of Motion. The equations of motion are defined in variational form, using the Hamilton's principle, as:

$$\int_{t_1}^{t_2}\left(-\int_V \delta\mathbf{S}_i^T\boldsymbol{\sigma}_i dV + \int_V \delta\left(\frac{1}{2}\rho\dot{u}_j^2\right)dV + \oint_\Gamma (\delta\bar{u}^T\bar{\tau} + \delta\varphi\bar{D})d\Gamma\right)dt = 0 \tag{2}$$

where i=1,…,6 and j=1,3; $\bar{\tau}$ and $\bar{D}$ are, respectively, the surface tractions and electric displacement, acting on the boundary surface Γ; $\bar{\mathbf{u}} = \begin{Bmatrix} \mathbf{u} \\ w \end{Bmatrix}$ is the generalized displacement vector. The first left hand side term in eq. (2) expresses electric enthalpy and dissipated energy in the piezoelectric structure, as mandated by the governing material eqs. (1). The

second LHS term is the kinetic energy of the piezoelectric structure. Considering a beam case, eq. (2) can be rewritten as,

$$\int_{t_1}^{t_2}(-\int_0^{L_x}\delta H_L dx-\int_0^{L_x}\delta W_{d_L} dx+\int_0^{L_x}\delta K_L dx+\int_0^{L_x}\delta \bar{\boldsymbol{u}}\,\bar{\boldsymbol{\tau}} dx)dt=0 \tag{3}$$

where δH_L, δW_{d_L} and δK_L are the variations of electric enthalpy, dissipated energy and kinetic energy of the piezoelectric laminate. The electric enthalpy includes the components of elastic strain energy, piezoelectric energy and electric energy. In the current beam case, in-plane and interlaminar shear strains are considered in the elastic field. The piezoelectric materials considered are monoclinic class 2 crystals with a poling direction coincident with the z-axis. Thus, the electric enthalpy in the m-th ply is expressed in variational form as,

$$\delta H_l=\int_{z_m}^{z_{m+1}}(\delta S_i Q_{c_{ij}} S_j-2\delta E_3 e_{31} S_1-\delta E_3 \varepsilon_{33} E_3)dz \tag{4}$$

where i,,j=1,5 and z_m, z_{m+1} indicate ply bottom and top surface, respectively. Similarly, the dissipated energy in a viscoelastic composite ply is expressed as:

$$\Delta W_{d_l}=\int_{z_m}^{z_{m+1}}\delta S_i Q_{c_{in}} \eta_{nj} S_j dz \tag{5}$$

where i,n,j=1,5.

Kinematic Assumptions. A typical laminate is assumed to be subdivided into n discrete layers as shown schematically in Fig. 1a, each discrete-layer may contain either a single ply, a sublaminate, or a subply of composite or piezoelectric material.

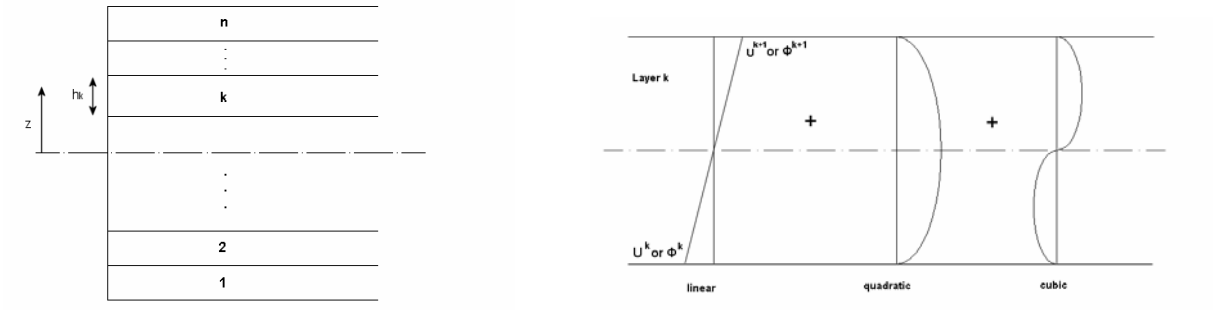

(a) **(b)**

Fig. 1. a) Typical laminate configuration analyzed with n-discrete layers. b) Assumed displacement and electric potential field through the thickness of each discrete layer.

Piecewise linear variation is first assumed through the laminate thickness for both in-plane displacement and electric potential fields, which maintains continuity across the discrete layer boundaries, while allowing for different slopes in each discrete layer. Parabolic and cubic variations in both fields are further considered through the thickness of each discrete layer (Fig. 1b). In this manner, the displacement and electric potential fields in the k-th discrete layer take the form:

$$
\begin{aligned}
u(x,z,t) &= U^k(x,t)\Psi_1^k(\zeta_k) + U^{k+1}(x,t)\Psi_2^k(\zeta_k) + \alpha_u^k(x,t)\Psi_3^k + \lambda_u^k(x,t)\Psi_4^k \\
w(x,z,t) &= w^o(x,t) \\
\varphi(x,z,t) &= \Phi^k(x,t)\Psi_1^k(\zeta_k) + \Phi^{k+1}(x,t)\Psi_2^k(\zeta_k) + \alpha_\varphi^k(x,t)\Psi_3^k + \lambda_\varphi^k(x,t)\Psi_4^k
\end{aligned}
\tag{6}
$$

where superscripts k=1,...,n indicates the discrete layer, and o the mid-plane. The first two terms in the right hand side describe the linear displacement and electric potential field, respectively; U^k, U^{k+1} and Φ^k, Φ^{k+1} are the in-plane displacements and the electric potentials, respectively, at the interfaces of each discrete layer [2]; Ψ_1^k, Ψ_2^k are linear interpolation functions through the layer thickness. Ψ_3^k, Ψ_4^k are the added quadratic, cubic interpolation functions, respectively, through the layer thickness. The last two terms in eq. (6) describe quadratic and cubic variations; α_u^k and λ_u^k are hyper-rotations in each discrete layer introduced by the quadratic and cubic terms, respectively; α_φ^k and λ_φ^k are additional electric degrees of freedom introduced by the quadratic and cubic approximations in the through-thickness electric potential field.; ζ_k is the local thickness coordinate of layer k [13].

Through-Thickness Strain and Electric Field. In the context of kinematic assumptions (6) the axial and shear strains S_1 and S_5 in each discrete layer are,

$$
\begin{aligned}
S_1^k &= U_{,x}^k\Psi_1^k + U_{,x}^{k+1}\Psi_2^k + (\alpha_u^k)_{,x}\Psi_3^k + (\lambda_u^k)_{,x}\Psi_4^k \\
S_5^k &= w_{,x}^o + (U^k\Psi_{1,\zeta_k}^k + U^{k+1}\Psi_{2,\zeta_k}^k + \alpha_u^k\Psi_{3,\zeta_k}^k + \lambda_u^k\Psi_{4,\zeta_k}^k)\frac{2}{h_k}
\end{aligned}
\tag{7}
$$

The comma in the subscripts indicates differentiation. In the axial strain equation, $U^k{}_{,x}$ and $U^{k+1}{}_{,x}$ represent contributions of the mid-layer strain and curvature, while the last two terms the contributions of hypercurvatures $\alpha^k{}_{,x}$ and $\lambda^k{}_{,x}$ in the discrete layer. In the interlaminar shear strain equation, the sum of the first three right hand side terms yields a constant shear term, while the last two terms provide a linear and a quadratic term through the thickness of the k-th layer. The electric field in the poling direction is,

$$
E_3^k = -(\Phi^k\Psi_{1,\zeta_k}^k + \Phi^{k+1}\Psi_{2,\zeta_k}^k + \alpha_\varphi^k\Psi_{3,\zeta_k}^k + \lambda_\varphi^k\Psi_{4,\zeta_k}^k)\frac{2}{h_k} \tag{8}
$$

The first two right hand side terms in the above equation yield a constant variation of the electric field in each discrete layer, while the last two terms further add a linear and a quadratic variation through the thickness of each discrete layer.

Discrete Layer Electric Enthalpy and Dissipated Energy. In the context of eqs. (4) and (5), the electric enthalpy and the dissipated energy in each discrete layer k is, respectively,

$$
\delta H^k = \sum_{n_p=m_b^k}^{m_t^k} \int_{\zeta_k^{m^k}}^{\zeta_k^{(m+1)^k}} (\delta S_i^k Q_{ij}^{m^k} S_j^k - 2\delta E_3^k e_{31}^{m^k} S_1^k - \delta E_3^k \varepsilon_{33}^{m^k} E_3^k)\frac{h_k}{2} d\zeta_k \tag{9}
$$

$$
\Delta W_d^k = \sum_{n_p=m_b^k}^{m_t^k} \int_{\zeta_k^{m^k}}^{\zeta_k^{(m+1)^k}} (\delta S_i^k Q_{in}^{m^k} \eta_{nj}^{m^k} S_j^k \frac{h_k}{2} d\zeta_k \tag{10}
$$

where i,,j,n=1,5 and m^k denotes the m-th ply in the k-th discrete layer; m_b^k and m_t^k denote bottom and top ply, respectively, of the k-th discrete layer.

Laminate Electric Enthalpy and Laminate Matrices. The electric enthalpy of the laminate is,

$$\delta H_L = \sum_{k=1}^{n} \delta H^k \tag{11}$$

The dissipated strain energy in the laminate is,

$$\Delta W_{d_L} = \sum_{k=1}^{n} \Delta W_d^k \tag{12}$$

Combining eqs. (4),(5),(9),(10),(11),(12) and taking into account the strain eqs. (7),(8) integrating through the thickness of each discrete layer and collecting the common terms, the laminate enthalpy is related to the laminate stiffness, piezoelectric and permittivity matrices and expressed in variational form as,

$$\delta H_L = \delta \mathbf{S}_1^T \left[A_L \right] \mathbf{S}_1 + \delta \mathbf{S}_5^T \left[As_L \right] \mathbf{S}_5 - 2\delta \mathbf{E}_3^T \left[P_L \right]^T \mathbf{S}_1 - \delta \mathbf{E}_3^T \left[L_L \right] \mathbf{E}_3 \tag{13}$$

and the laminate dissipated energy is related to the laminate in-plane and shear damping matrices as,

$$\Delta W_{d_L} = \delta \mathbf{S}_1^T \left[A_{d_L} \right] \mathbf{S}_1 + \delta \mathbf{S}_5^T \left[As_{d_L} \right] \mathbf{S}_5 \tag{14}$$

In the above equations $\mathbf{S}_1, \mathbf{S}_5$ and $\mathbf{E}_3$ are the laminate normal and shear strain vectors and the electric field vector, respectively, given by:

$$\begin{aligned}
\mathbf{S}_1 &= \left\{ U^1_{,x}, ..., U^{n+1}_{,x}, (\alpha_u^1)_{,x}, ..., (\alpha_u^n)_{,x}, (\lambda_u^1)_{,x}, ..., (\lambda_u^n)_{,x} \right\} \\
\mathbf{S}_5 &= \left\{ w^o_{,x}, U^1, ..., U^{n+1}, \alpha_u^1, ..., \alpha_u^n, \lambda_u^1, ..., \lambda_u^n \right\} \\
\mathbf{E}_3 &= \left\{ \Phi^1, ..., \Phi^{n+1}, \alpha_\varphi^1, ..., \alpha_\varphi^n, \lambda_\varphi^1, ..., \lambda_\varphi^n \right\}
\end{aligned} \tag{15}$$

and $\left[A_L \right], \left[As_L \right], \left[P_L \right], \left[L_L \right], \left[A_{d_L} \right], \left[As_{d_L} \right]$ are the laminate in-plane stiffness, interlaminar shear stiffness, piezoelectric, permittivity, in-plane damping and interlaminar shear damping matrices, respectively.

Through-Thickness Compatibility. The displacement continuity at ply interfaces is self-imposed by the kinematic assumptions (6). Although, the compatibility of shear stresses on the layer interfaces and free surfaces is weakly maintained through the equations of equilibrium, shear stress compatibility conditions may be also explicitly imposed. In the latter case, transverse shear stresses should be continuous between adjacent layers, and equal to surface tractions τ_5^L, τ_5^U at the free edges, that is,

$$\begin{aligned}
&\sigma_5^k(\zeta_k = 1) = \sigma_5^{k+1}(\zeta_{k+1} = -1) \\
&\sigma_5^1(\zeta_1 = -1) = \tau_5^L \\
&\sigma_5^n(\zeta_n = 1) = \tau_5^U
\end{aligned} \tag{16}$$

where n is the upper discrete-layer. Imposition of these n+1 linear equations results in additional advantages: (1) it enables prediction of shear stresses at the ply interface; and (2) it yields a set of linear equations, thus, relating n+1 of the laminate structural DOFs to the

remaining ones. The former were selected to be all λ_u^i, i=1,…,n and the α_u^n and are eventually compensated. The shear stress compatibility equations, thus take the following form,

$$\begin{Bmatrix} \alpha_u^n \\ \lambda_u^i \end{Bmatrix} = [\boldsymbol{R}] \begin{Bmatrix} w_{,x} \\ \mathbf{U}^j \\ \alpha_u^k \end{Bmatrix} \tag{17}$$

where i=1,…,n, j=1,…,n+1, k=1,…,n-1; [***R***] is the structural reduction matrix, having dimensions (n+1)x(2n+1) [14]. Inclusion of eq. (17) into the governing laminate equations leads to the elimination of n+1 laminate DOFs.

Structural Piezoelectric Response

Finite Element Formulation. A beam finite element is developed, which incorporates the theoretical framework presented. The compatibility equations (16) or (17) imply that in order to maintain continuity in the eliminated hyper-rotations λ^i (i=1,…,n) and a^n, the slope of the transverse displacement $w^o_{,x}$ should also remain continuous along element boundaries, hence a requirement is imposed for C_1 continuity on w^o by the shear stress compatibility equations. C_1 continuous shape functions H(x) were implemented in the local approximation of the transverse displacement w^o, while C_o shape functions N(x) were used for the remaining DOFs. The use of C_1 shape functions also results in continuity in the constant shear strain component of eq. (7) at the nodes. In this manner, the developed element yields continuity of the constant shear strain component at the nodes and continuity of σ_5 at ply interfaces through the thickness. A 2-node beam element was developed and encoded employing cubic Hermitian polynomials for the transverse deflection and linear interpolation functions for all other variables [13].

The coupled dynamic piezoelectric system can be expressed in a discrete matrix form [5]:

$$\begin{bmatrix} [M_{uu}] & 0 \\ 0 & 0 \end{bmatrix} \begin{Bmatrix} \{\ddot{u}\} \\ \{\ddot{\varphi}^F\} \end{Bmatrix} + \begin{bmatrix} [C_{uu}] & 0 \\ 0 & 0 \end{bmatrix} \begin{Bmatrix} \{\dot{u}\} \\ \{\dot{\varphi}^F\} \end{Bmatrix} + \begin{bmatrix} [K_{uu}] & [K_{u\varphi}^{FF}] \\ [K_{\varphi u}^{FF}] & [K_{\varphi\varphi}^{FF}] \end{bmatrix} \begin{Bmatrix} \{u\} \\ \{\varphi^F\} \end{Bmatrix} = \begin{Bmatrix} \{F(t)\} - [K_{u\varphi}^{FA}]\{\varphi^A\} \\ \{Q^F\} - [K_{\varphi\varphi}^{FA}]\{\varphi^A\} \end{Bmatrix} \tag{18}$$

Submatrices $[K_{uu}]$, $[K_{u\varphi}]$ and $[K_{\varphi\varphi}]$ indicate the elastic, piezoelectric and permittivity matrices of the structure; superscripts F and A indicate, respectively, sensory (free) and active (applied) electric potential components; {P} is the applied mechanical forces vector and $\{Q^F\}$ is the applied electric charge at the sensors, which is assumed to be zero (open circuit conditions). Additional manipulation of eqs. (18) results in the following uncoupled equations for the structural displacements and sensory voltages respectively,

$$\begin{aligned} &[M_{uu}]\{\ddot{u}\} + [C_{uu}]\{\dot{u}\} + ([K_{uu}] - [K_{u\varphi}^{FF}][K_{\varphi\varphi}^{FF}]^{-1}[K_{\varphi u}^{FF}])\{u\} = \{F(t)\} - [K_{u\varphi}^{FA}]\{\varphi^A\} \\ &\{\varphi^F\} = -[K_{\varphi\varphi}^{FF}]^{-1}[K_{\varphi u}^{FF}]\{u\} \end{aligned} \tag{19}$$

Solution of the above system yields the coupled electromechanical response of the piezoelectric beam structure. The participation of actuators in the modal response of the structure can be accomplished by considering that the active voltages are related to the structural degrees of freedom as,

$$\{\varphi^A\} = [G]\{u\} \tag{20}$$

where [G] is the gain matrix. Substituting eq. (20) in the structural system (19) includes the effect of active voltage on the damped modal response of the beam. The practical purpose of equation (20) is to be able to actively shear the damping layer restrained between actuator and plies by applying proper electric feedback.
Assuming free harmonic motion, the above system in the frequency domain can be written in a simplified form,

$$-\omega^2[\mathbf{M}]\{\mathbf{V}\} + j[\mathbf{C}]\{\mathbf{V}\} + [\mathbf{K}]\{\mathbf{V}\} = 0 \tag{21}$$

where [**M**], [**C**] and [**K**] are the inertia, damping and stiffness matrices of the beam, respectively and {**V**} are the amplitude vectors.
Eq. (21) can be solved directly, to yield the complex eigenvalues of the system, from which modal frequencies and damping can be extracted. Alternatively, using the dissipated energy approach, the modal loss factor associated with the m-th order mode η_m will be the ratio of dissipated to stored strain modal energy of the m-th mode

$$\eta_m = \frac{\int_0^{L_x} \Delta W_{Lm} dx}{\int_0^{L_x} W_{Lm} dx} \tag{22}$$

The numerical solution of eq. (21) for [**C**=0] provides the undamped natural frequencies and the modal displacement vectors of the beam. The modal loss factor of the beam is then calculated from the ratio of the respective dissipated and maximum stored energies:

$$\eta_m = \frac{\mathbf{V}_m^T[\mathbf{C}]\mathbf{V}_m}{\mathbf{V}_m^T[\mathbf{K}]\mathbf{V}_m} \tag{23}$$

3. RESULTS AND DISCUSSION

The damped dynamic characteristics of a sandwich beam with composite faces, foam core and piezoelectric layers are studied using the developed model. Modal displacements, electric potential, strains, electric field and stresses are compared to those obtained using a linear layerwise beam finite element [2]. The effect of constrained damping layers on modal response and damping is predicted and the active enhancement of damping caused by the application of electric potential at the piezoelectric layers is also investigated. The mechanical properties of all materials considered are listed in Table 1.

Table 1. Mechanical, Piezoelectric and dielectric properties of materials considered.

	Gr/Ep composite	**Klegecell R foam**	**3M 110 polymer**	**PZT-4**
E_{11} (GPa)	126.0	35.0 e-3	113.0 e-3	81.3
G_{13} (Gpa)	3.4	12.3 e-3	38.0 e-3	25.6
v_{13}	0.28	0.40	0.49	0.31
d_{31} (10^{-12} m/V)	0	0	0	-122.0
ε_{33} (10^{-9} farad/m)	26.6e-3	26.6e-3	26.6e-3	11.53
η_{l1} (%)	0.08	2.4	16.0	0
η_{l5} (%)	1.1	3.0	16.0	0

[pzt-4/0/foam]$_S$ Sandwich Beam. A simply-supported sandwich beam with Graphite-Epoxy composite faces and foam core, having piezoelectric layers attached at the faces, is considered. The beam has a length of 1000 mm and the thicknesses of the sublaminates are 2.5 mm for each composite face, 30 mm for the foam core and 1 mm for each piezoelectric layer. The top and bottom surface of the piezoelectric layers are grounded. The beam is modeled using 5 discrete layers through the thickness, namely 1 for each piezoelectric layer, 1 for each composite face and 1 for the foam core, whereas 50 discrete layers are used in the linear layerwise model. Figs. 2a-h illustrate predicted through-thickness distributions of maximum axial displacement, electric potential, axial strain, interlaminar shear strain, electric field, axial stress, interlaminar shear stress and electric displacement, respectively, for the three first bending modes. The linear layerwise model predicts strain, electric field, stress and electric displacement at the middle of each discrete layer, whereas the predictions of the high-order layerwise model are at the ply interfaces. Excellent correlation is observed between the two models for all variables studied. The use of high-order approximation for axial displacement and electric potential within each discrete layer enables accurate capturing of parabolic distributions of interlaminar shear stress at the composite faces and electric potential at the piezoelectric sensors, respectively, using one discrete layer for each face and sensor. Moreover, piecewise linear distributions are accurately predicted using a minimum number of discrete layers, indicating the efficiency of the current methodology.

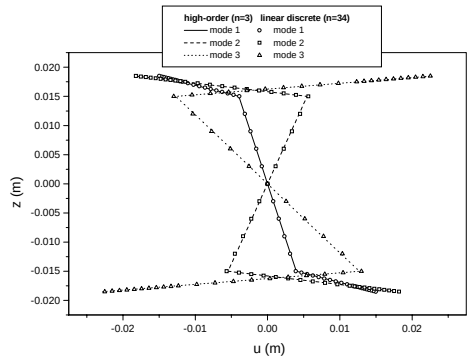

(a)

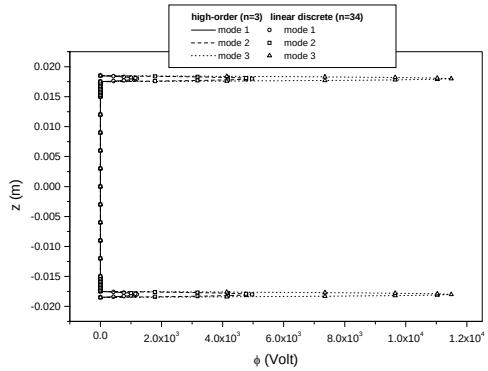

(b)

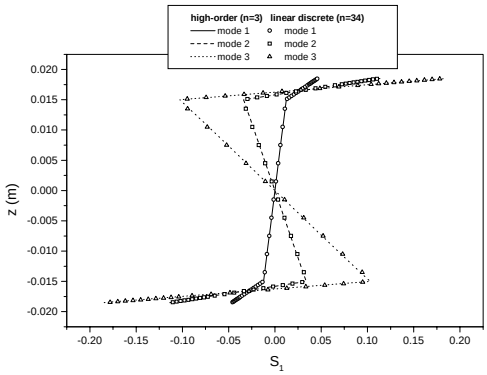

(c)

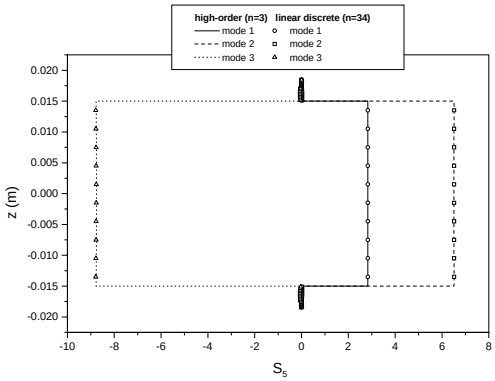

(d)

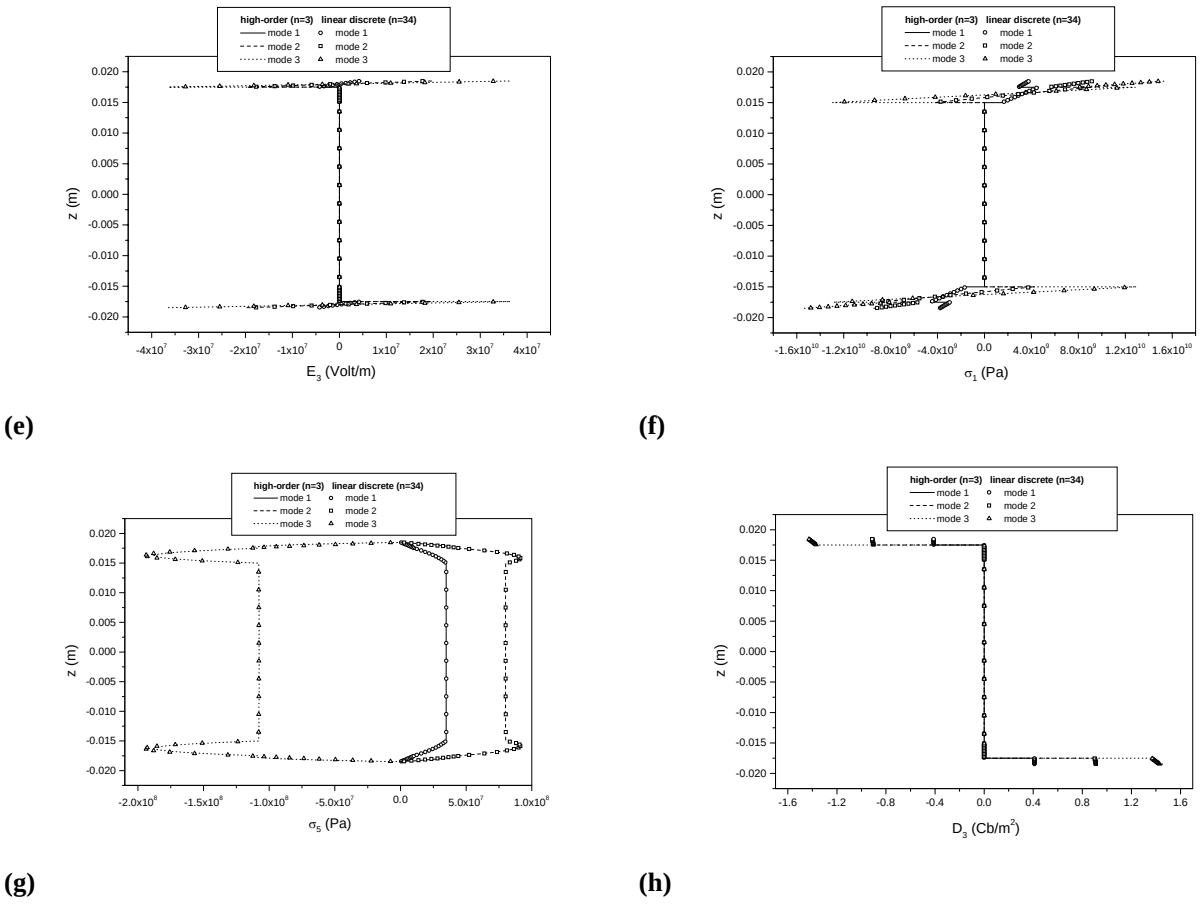

Fig. 2. Through-thickness distribution of modal a) displacement, b) electric potential, c) axial strain, d) interlaminar shear strain, e) electric field, f) axial stress, g) interlaminar shear stress, h) electric displacement .

Modal damping values for the 8 first bending modes are shown in Fig. 3a. As shown in Figs. 2d and 2g, the interlaminar shear strain in the foam core increases in the higher bending modes, whereas the interlaminar shear stresses are higher at the faces after the fundamental bending mode. Higher shear strain in the foam core is expected to yield increasing damping predictions for higher bending modes, however it seems that there is an overlapping between face and core damping. The damping of the core is dominant only in the first two modes, whereas damping of the faces dominates in the remaining modes, leading to a reduction of damping, since damping of the stiff restraining faces is negligible. The addition of an interlaminar damping layer between piezoelectric layer and composite face increases the shear strain of the sandwich's face, as illustrated in Fig. 3b, where the modal shear strain of the fifth bending mode with and without the compliant layer is shown. It also leads to an increase in damping of the sandwich beam, as shown in Fig. 3a.

Based on eq. (20), the electric potential at the piezoelectric layers can be actively tailored in order to improve the damping of the sandwich beam by increasing the interlaminar shear strain. As mandated from the second of eqs. (7), the structural degrees of freedom related to the interlaminar shear strain are U^i and $w_{,x}$ and can be affected through [G]. Fig. 4 shows the variation of interlaminar shear strain of the fundamental bending mode through the thickness at three-quarters of the length for the passive and an active configuration, which assumes grounded inner faces of the piezoelectric layers and applied voltage at their top surfaces related to $w_{,x}$ through a gain of -8e3. The fundamental mode is the only one affected by this active configuration, which leads to an improvement of 22% in modal damping.

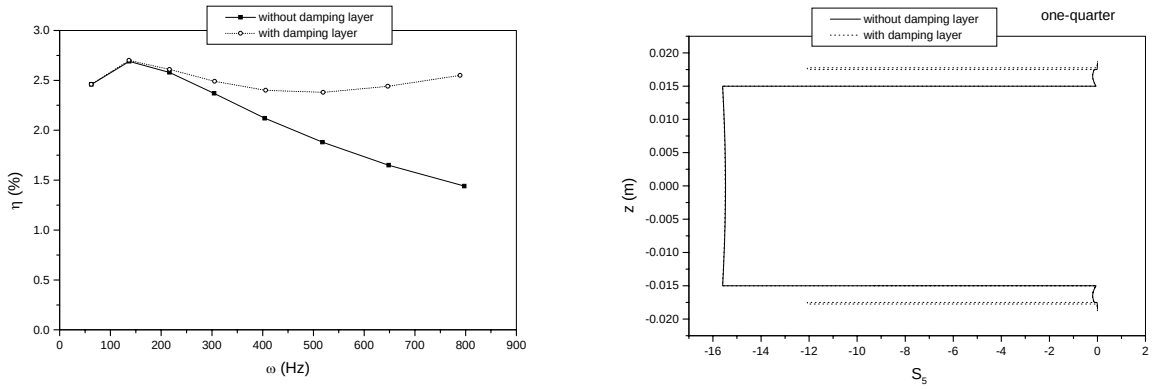

(a) **(b)**

Fig. 3. Effect of interlaminar compliant layers on **(a)** modal damping of the first eight bending modes, **(b)** through-thickness distribution of interlaminar shear strain of the fifth bending mode.

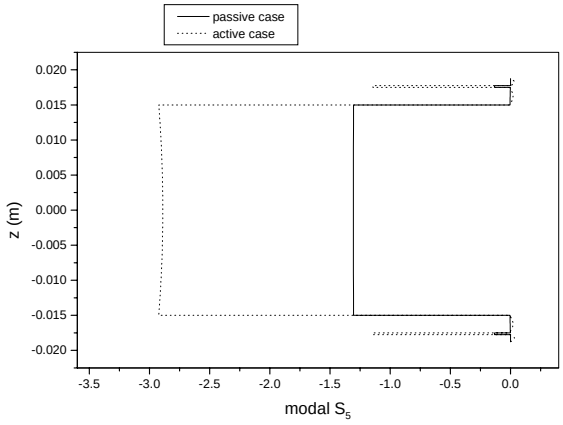

Fig. 4. Active increase of interlaminar shear strain through-thickness for the fundamental bending mode.

4. SUMMARY

Integrated discrete-layer mechanics and a finite element were presented for predicting the coupled dynamic response of sandwich beams with piezoelectric layers. A high-order layerwise piezoelectric theory was developed, which satisfies through-thickness compatibility of interlaminar shear stress and allows for higher order distribution of displacement and electric potential in each discrete layer. The theoretical model was incorporated in a new finite element with continuous interlaminar shear strains and stresses at nodes, which predicts stress and strain at the ply interfaces. The damped dynamic characteristics of a sandwich beam with composite faces and piezoelectric layers were predicted. Validation with a linear layerwise piezoelectric model illustrated the efficiency of the developed formulation, which accurately captures the through thickness distribution of modal variables using a minimum number of discrete layers. The damping of the sandwich beam was enhanced by the addition of interlaminar compliant layers between piezoelectric layer and composite face, due to the increase of interlaminar shear strain at the faces, and it was further improved by actively using the piezoelectric layers.

Future work will focus on the extension of the developed theoretical background in plate structures and the inclusion of shear piezoelectric coupling, in order to predict the local/global damped dynamic response in the case of axially polarized piezoelectric layers.

References

1. **Saravanos, D.A.** and **Heyliger, P.R.,** "Coupled layerwise analysis of composite beams with embedded piezoelectric sensors and actuators", *Journal of Intelligent Material Systems and Structures*, **6**/3 (1995), 350-363.
2. **Heyliger, P.R., Ramirez, G.** and **Saravanos, D.A.,** "Coupled discrete-layer finite-element models for laminated piezoelectric plates", *Communications in Numerical Methods in Engineering*, **10** (1994), 971-981.
3. **Heyliger, P.R.** and **Brooks, S.P.,** "Exact solutions for piezoelectric laminates in cylindrical bending", *Journal of Applied Mechanics*, **63**/4 (1996), 903-910.
4. **Heyliger, P.R.** and **Saravanos, D.A.,** "Exact free-vibration analysis of laminated plates with embedded piezoelectric layers", *Journal of the Acoustical Society of America*, **98**/3 (1995), 1547-1557.
5. **Saravanos, D.A.,** "Coupled mixed-field laminate theory and finite element for smart piezoelectric composite shell structures", *AIAA Journal*, **35**/8 (1997), 1327-1333.
6. **Gu, H., Chattopadhyay, A., Li, J.** and **Zhou, X.,** "A higher order temperature theory for coupled thermo-piezoelectric-mechanical modeling of smart composites", *International Journal of Solids and Structures*, **37**/44 (2000), 6479-6497.
7. **Kim, H.S., Zhou, X.** and **Chattopadhyay, A.,** "Interlaminar stress analysis of shell structures with piezoelectric patch including thermal loading", *AIAA Journal*, **40**/12 (2002), 2517-2525.
8. **Cho, M.** and **Oh, J.,** "Higher order zig-zag theory for fully coupled thermo-electric-mechanical smart composite plates", *International Journal of Solids and Structures*, **41**/ (2003), 1331-1356.
9. **Zhang, H.D**. and **Sun, C.T.,** "Formulation of an Adaptive Sandwich Beam", *Smart Materials and Structures*, **5**/6 (1996), 814-823.
10. **Trindade, M.A., Benjeddou A.** and **Ohayon, R.,** "Finite element modelling of hybrid active-passive vibration damping of multilayer piezoelectric sandwich beams-part I: Formulation", *International Journal for Numerical Methods in Engineering*, **51**/7 (2001), 835-854.
11. **Raja, S., Prathap, G.** and **Sinha, P.K.**, "Active vibration control of composite sandwich beams with piezoelectric extension-bending and shear actuators", *Smart Materials and Structures*, **11**/1 (2002), 63-71.
12. **Vel, S.S.** and **Batra, R.C.,** "Exact solution for rectangular sandwich plates with embedded piezoelectric shear actuators", *AIAA Journal*, **39**/7 (2001), 1363-1373.
13. **Plagianakos, T.S.** and **Saravanos, D.A.,** "Analysis of adaptive sandwich composite beams with piezoelectric actuators and sensors using coupled high-order layerwise mechanics", *AIAA/ASME/ASCE/AHS/ASC SDM Conference and Adaptive Structures Forum 2004, Palm Springs, California.*
14. **Plagianakos, T.S.** and **Saravanos, D.A.,** "High-order layerwise mechanics and finite element for the damped dynamic characteristics of sandwich composite beams", submitted to the *International Journal of Solids and Structures*.